Proceedings of the ASME 2010 3rd Joint US-European Fluids Engineering Summer Meeting and 8th International Conference on Nanochannels, Microchannels, and Minichannels
FEDSM-ICNMM2010
August 1-5, 2010, Montreal, Canada

FEDSM-ICNMM2010-30984

INVESTIGATION OF THE BEHAVIOR OF VENTILATED SUPERCAVITIES

Ellison Kawakami
University of Minnesota
Saint Anthony Falls Laboratory
Email: kawa0054@umn.edu

Roger E. A. Arndt
University of Minnesota
Saint Anthony Falls Laboratory
Email: arndt001@umn.edu

ABSTRACT

A study has been carried out at the Saint Anthony Falls Laboratory (SAFL) to investigate various aspects of the flow physics of a supercavitating vehicle. For the experimental work presented here, artificial supercavitation behind a sharp-edged disk was investigated for various model configurations. Results regarding supercavity shape, closure, and ventilation requirements versus Froude number are presented. Conducting experiments in water tunnels introduces blockage effects that are not present in nature. As a result, effects related to flow choking are also discussed. Various methods for computing ventilated cavitation number, including direct measurement of pressure, Laser Doppler Velocimetry, and use of previous numerical results, were compared. Results obtained are similar in character to previous results from various authors, but differ significantly in measured values. Supercavitation parameters, especially the minimum obtainable cavitation number are strongly affected by tunnel blockage

INTRODUCTION

Drag reduction and/or speed augmentation of marine vehicles by means of supercavitation has been a topic of great interest. When supercavitation is achieved, a large vapor bubble encompasses the vehicle. There are two ways in which a marine vehicle can achieve supercavitation. The first method, termed natural supercavitation, occurs when the velocity of the vehicle is high enough tp ensure that a vapor cavity is sufficiently large enough to envelope the vehicle. In the second method, termed artificial, or ventilated, supercavitation, a supercavity is generated by blowing non-condensable gas into the low-pressure region near the nose of the vehicle. This paper focuses on the study of the second method, artificial supercavitation.

Various researchers have conducted experiments as well as numerical simulations on several aspects of supercavities. Semenenko [1] and Savchenko [2] pointed out two main issues that arise for axisymmetric, ventilated supercavities in horizontal flow. The first is the mode of evacuation of the air at the rear of the cavity, and the second is the deformation of the cavity under the influence of gravity. Three modes of air leakage have been observed by various authors. These modes are summarized by Franc and Michel [3]. In the first mode of air leakage, termed the re-entrant jet regime, the tail of the supercavity is filled with foam, which is periodically rejected in the form of unstable, toroidal vortices. In the second form of gas leakage, termed the twin vortex regime, two hollow vortex tubes exist at the tail end of the cavity, which is significantly affected by gravity. Supercavities in the twin vortex regime are much longer than those in the re-entrant regime. The third form of gas leakage corresponds to pulsating cavities that occur when there is a high flowrate coefficient. The first mode of gas leakage is predicted to occur when $\sigma_c Fr < 1$ and the second mode when $\sigma_c Fr > 1$. The third mode of gas leakage depends on the parameter $\beta = \sigma_c/\sigma_v$ [4]. Paryshev predicted that a pulsating cavity would be present when $\beta > 2.64$.

PREVIOUS RESULTS

The study of ventilated flows at SAFL was planned as an interactive experimental/numerical study. The first configuration studied had a replaceable sharp edged disk that was mounted on the upstream nose of the model. The model had special ventilation ports for injection of air behind the cavitator to create the supercavity. Choking was taken into account in the design of the test body. Early studies (Wosnik et al [5]) were focused on aspects of the flow physics of the supercavity around the test body, generated by the cavitator. Digital strobe photography was utilized to describe cavity shape and re-entrant jet interaction. Ventilation gas

requirements to create and sustain an artificial cavity were studied at various Froude numbers. Froude number was varied in two ways; the first was to vary the tunnel velocity, and the second was to vary the size of the cavitator on the test body. It was found that the strut shape, which the test body was mounted on, critically affects the air demand through cavity-strut wake interaction.

Some of the detailed measurements of Wosnik et al. [5] are shown in Figure 1. The data were collected for two cavitator sizes, and two mounting strut types, at a given same Froude number. The data are presented in the form of air entrainment coefficient, C_q, versus ventilated cavitation number, σ_c. Note that the minimum cavitation number for the larger disk is higher than for the smaller disk. Also note that at the minimum cavitation number for a given cavitator, further increase in ventilation number does not further decrease the cavitation number. Schauer [6] suggested that this is an effect of blockage. A second consideration is that this behavior is due to a transition from the first method of gas leakage to the second form of gas leakage. The issue is further complicated by the difficulty in measuring the cavitation number with the test body used. Wosnik et al. utilized the results of Brennen [7] to infer the cavitation number from measurements of the cavitation shape. This procedure introduced a question of uncertainty in the results. The effects of the strut used to mount the test body on the closure of the supercavity also generated questions. This work provided a basis for further work, described in this paper.

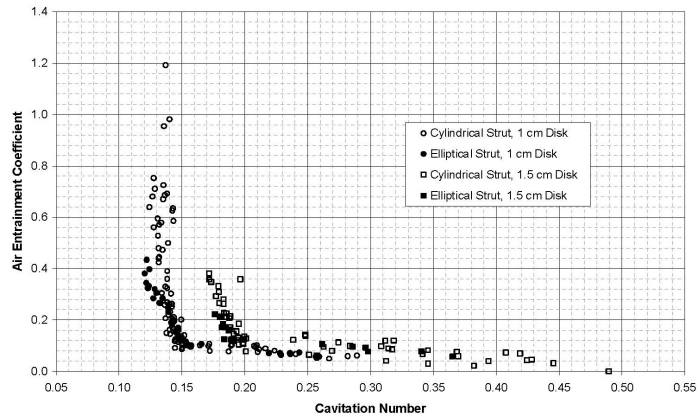

Figure 1. Air entrainment data for both disks and struts. Cavitation number computations were refined using data of Brennen [7]. From Wosnik et al. [5].

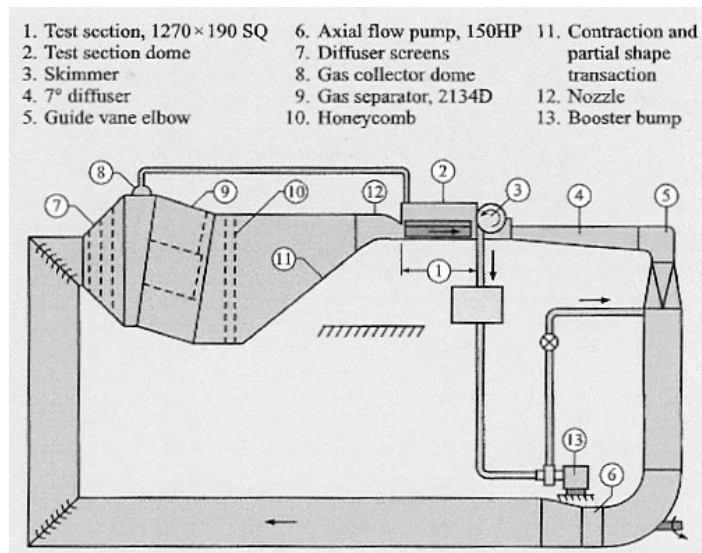

Figure 2. SAFL tunnel schematic.

EXPERIMENTAL SETUP

The current study was conducted in the high-speed water tunnel at SAFL. This water tunnel is a recirculating, closed-jet facility with absolute pressure regulation. The tunnel is capable of velocities in excess of 20 m/s. The test section measures 0.19m (W) x 0.19m (H) x 1m (L), and is fitted with observation windows on three sides. A special design of the tunnel allows for the removal of large quantities of air during ventilation experiments, allowing for conduction of experiments with little to no effect on test section conditions. The tunnel has a minimum turbulence level of 0.4% at 10 m/s. Figure 2 provides a schematic of the SAFL water tunnel

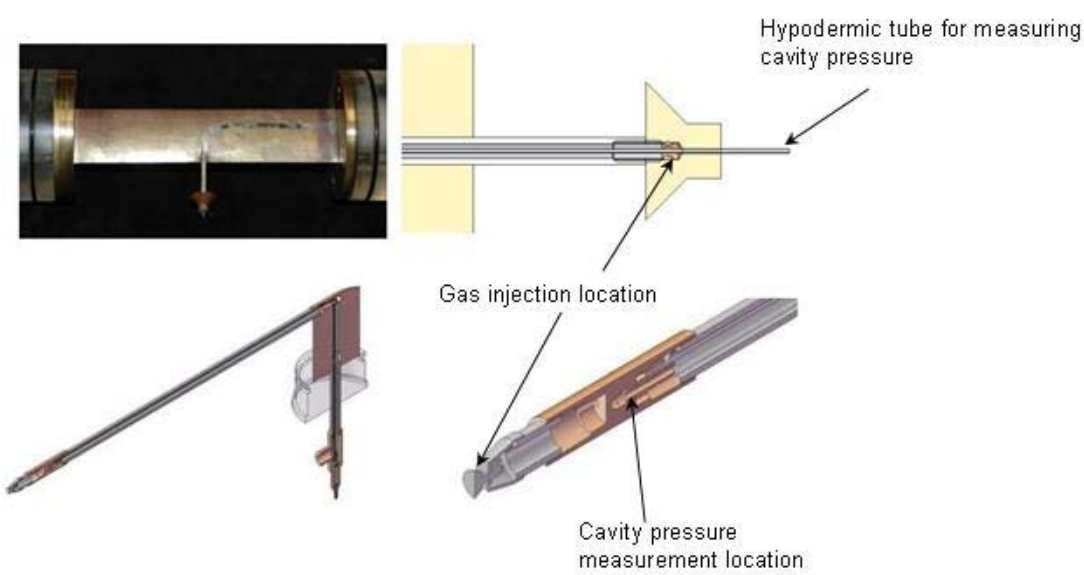

Figure 3. Backward facing model (top) and forward facing model (bottom).

To address the questions from the previous experimental work, experiments were conducted on new test bodies, which can be seen in Figure 3. The forward facing model, cavitator upstream of the mounting strut, has a long, hollow tube between the cavitator and mounting strut in an effort to eliminate the strut influence on the closure of the supercavity. The backward facing model, cavitator downstream of the mounting strut, eliminated the presence of a body inside the supercavity completely. Two cavitator sizes, 10mm and 20mm, were tested for both models. Both models also had the capability of directly measuring the pressure inside the supercavity.

RESULTS

Figure 4 shows a comparison of Brennen's numerical predictions to data obtained from direct measurement of the cavity pressure for the backward facing model. Several aspects of the plot are noteworthy. Given a cavitator size, it was found that as the Froude number increased, the minimum cavitation number, corresponding to a clear, stable cavity, decreased. For both sizes of cavitators, it was observed that at lower Froude numbers, the experimental data did not show strong support for predicting cavitation number based on cavitator diameter and half-length (Brennen's method [7]), while at higher Froude numbers, there was strong agreement. Similar results were observed with the forward facing model. This is due to Brennen's assumption of infinite Froude number for his calculations. In Figures 4 and 5 it is also worth noting that the data corresponds only to pressure readings when a clear supercavity was present at various ventilation rates (twin vortex regime). This accounts for the clustering of data points for a given Froude number, which will be discussed further below.

The results from Figure 4 and 5 were not unexpected as Brennen's numerical predictions assumed an infinite Froude number. It was found, however, that an infinite Froude number is not necessary to utilize Brennen's numerical predictions. Earlier work by Tulin [8] indicated that the minimum cavitation number was a function of the blockage ratio as indicated in Figure 6. Tulin, similar to Brennen, assumed an infinite Froude number for his calculations. In reality, the minimum cavitation number is a function of both the blockage ratio, and the Froude number. This is shown in Figure 7. The cavitation number from experimental data is normalized by the minimum value for a given blockage ratio, predicted by Tulin (Figure 6). In Figure 7, the results from both cavitators are shown. As the Froude number increased, both sets of data approached unity and the agreement between Brennen's predictions and experimental data also increased. This indicated that as long as the normalized minimum cavitation number is close to unity, Brennen's model could be used to predict the ventilated cavitation number for a given flow rate and Froude number.

The ability to predict the cavitation number using Brennen's predictions is very advantageous for models where direct measurement of the pressure inside the supercavity is not possible. A disadvantage to Brennen's method is that the cavitation number can only be obtained after post-processing images acquired during the experiment. This process can be lengthy and introduces potential sources of error.

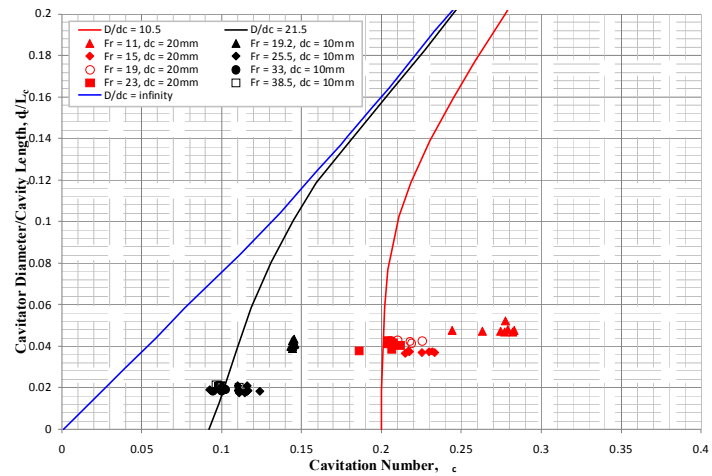

Figure 4. Backward facing model comparison of experimental data at various Froude numbers to Brennen's numerical predictions at infinite Froude number[7]. Calculations are shown with solid lines. Disk diameters of 10mm and 20mm correspond to D/d_c values of 21.5 and 10.5, respectively.

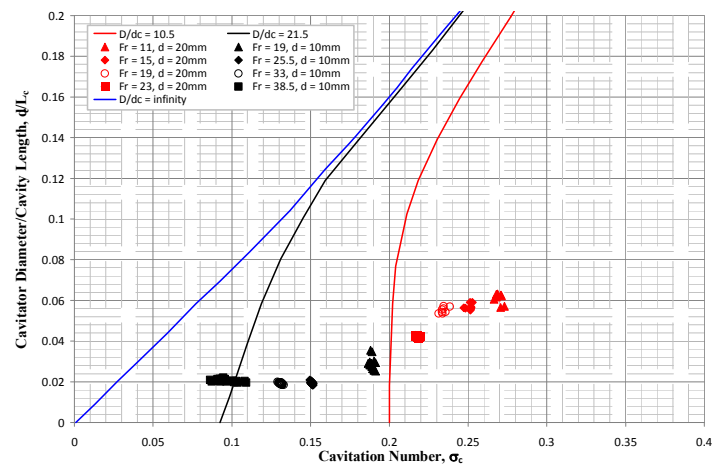

Figure 5. Forward facing model comparison of experimental data at various Froude numbers to Brennen's numerical predictions at infinite Froude number[7]. Calculations are shown with solid lines. Disk diameters of 10mm and 20mm correspond to D/d_c values of 21.5 and 10.5, respectively.

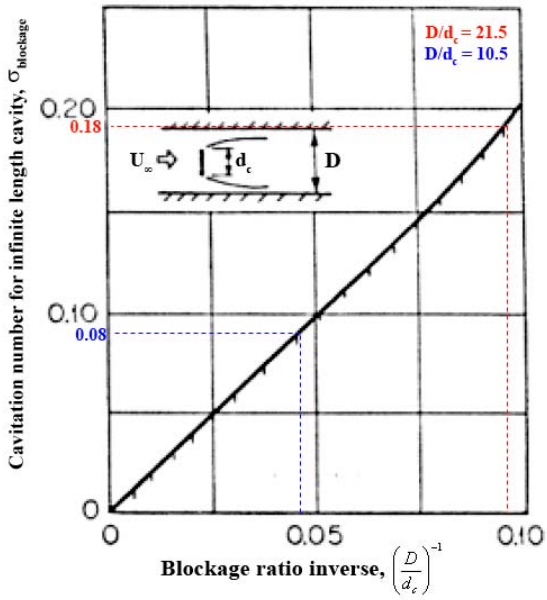

Figure 6. Tulin [8] predictions for minimum cavitation number as a function of the inverse of the blockage ratio.

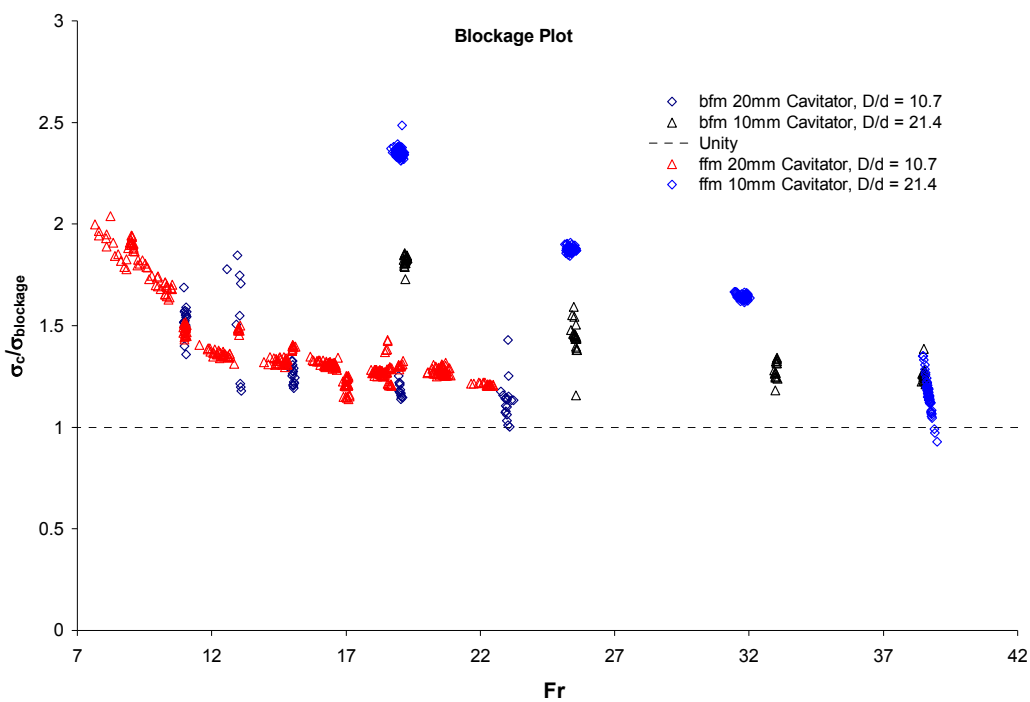

Figure 7. Ratio of minimum cavitation number obtained experimentally to minimum cavitation number predicted by Tulin [8]. Data are for cavitator diameters of 10 and 20 mm.

Another method for finding the cavitation number is to use Laser Doppler Velocimerty (LDV). Applying the Bernoulli equation for steady flow, the cavitation number can be expressed by the following equation

$$\sigma_c = \left(\frac{U_c}{U_\infty}\right)^2 + 2\left(\frac{gh}{U_\infty^2}\right) - 1$$

where U_c is the fluid velocity at the surface of the cavity at the maximum supercavity diameter. The immediate advantage to this equation for the cavitation number is that no pressure measurements are necessary. Figure 8 provides a comparison of the two methods for measuring the ventilated cavitation number. At lower values of Froude number, the ratio between the ventilated cavitation number and the minimum value due to blockage is closer to unity than the ratio found using a pressure transducer. At higher Froude numbers, the two methods show more agreement. The reason for the difference in the empirical data for the two methods at lower Froude numbers is presently unknown and is being investigated further. Figure 8 provides a comparison for only one of the configurations tested. Results for the other configurations tested are preliminary and are being explored further.

Figures 9 and 10 show a comparison the air entrainment coefficient against the cavitation number using the three methods previously discussed. For these experiments the ventilation rate was increased in step increments, gathering data and digital images at each step. At a certain ventilation rate, depending on the Froude number, the cavity would transition from a short, unsteady, and foamy cavity (re-entrant jet) to a long, clear, and steady supercavity (twin-vortex). Once a clear, stable cavity was formed, the cavitation number reached a minimum and did not increase or decrease significantly with an increase or decrease in ventilation. It should also be noted that once a clear, stable cavity was formed, the ventilation rate could be lowered beyond the transition value without the collapsing cavity. This behavior was observed for both models.

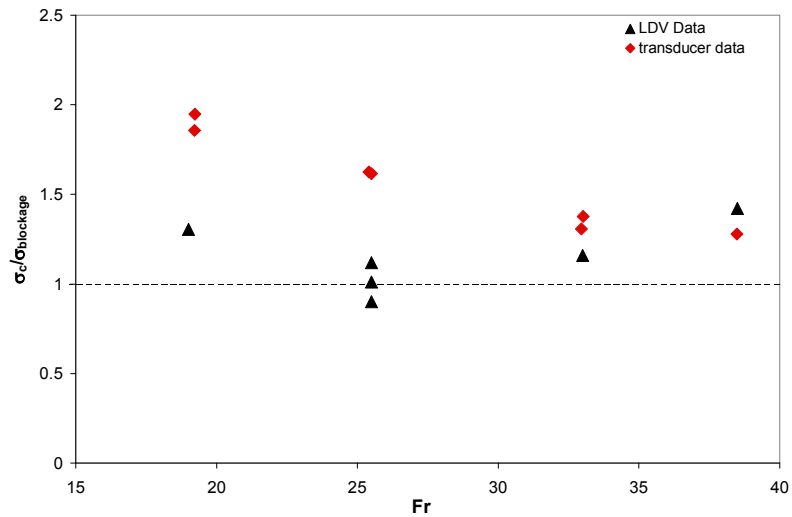

Figure 8. Comparison of results from LDV and pressure transducer data for the backward facing model with a 10mm cavitator.

A significant difference between the two models is that the backward facing model's transition from a foamy to a clear supercavity was at a lower ventilation rate than the forward facing model for similar conditions. The presence of a body inside the supercavity results in an increase in the ventilation rate at which the cavity will transition from a short, foamy cavity to a long, clear cavity.

The three methods showed good agreement with each other for the conditions shown in Figures 9 and 10. It should be noted that in Figure 9 only the Brennen predictions are shown for cavitation numbers greater than the minimum. This is due to the fact that the unsteady, foamy cavity made pressure measurements inside the cavity unreliable. To emphasize the affect of the unsteadiness of the short foamy cavities, Figure 10 depicts that at the same ventilation rate, during the same run, there is a significant difference in cavitation number obtained from the pressure transducer.

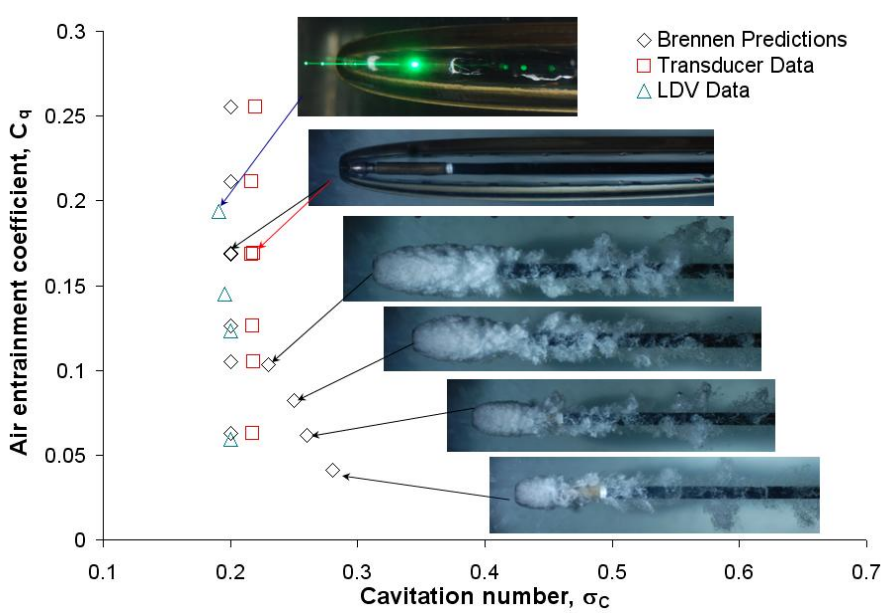

Figure 9. Forward facing model comparison of various measurement techniques for measuring cavitation number. Fr = 23, d_c = 20mm.

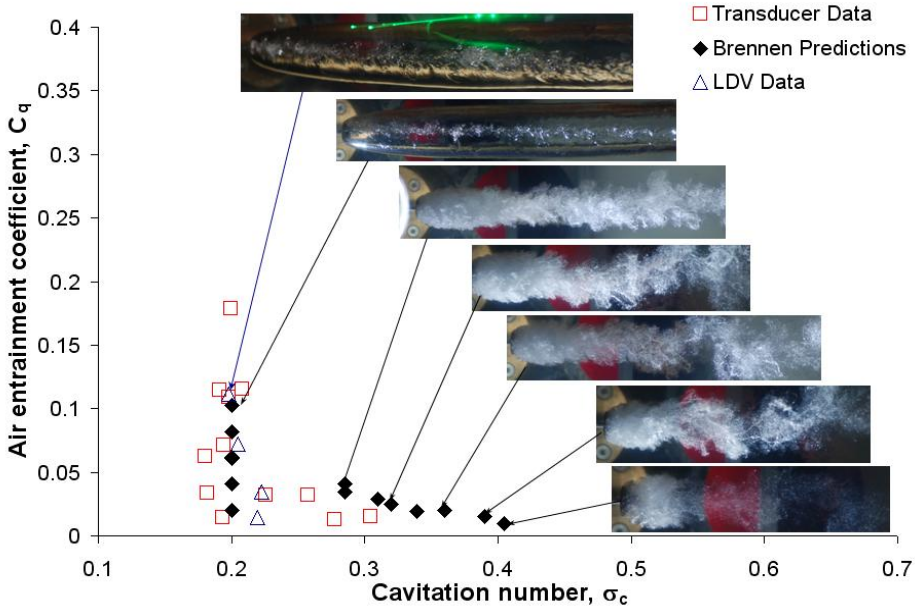

Figure 10. Backward facing model comparison of various measurement techniques for measuring cavitation number. Fr = 23, d_c = 20mm

A detailed examination was made of cavity closure, an essential element in the physics of the ventilation demand. For all experiments, the product $\sigma_c Fr$, where the cavitator diameter was used as the characteristic length when computing the Froude number, was always much greater than one, which various authors predict for the re-entrant jet regime. This was rarely the case, as the twin-vortex entrainment mechanism was dominantly observed (Figure 11). An unexpected observation found that while the supercavity itself was stable (constant diameter and length), the vortex pair at the tail of the supercavity was not. As seen in Figure 11, at one instant in time, a vortex core is present, while at a later time, there is a vortex collapse followed by a reformation of a vortex core. This was an ongoing process for a given set of conditions and was observed in both models.

A stable re-entrant jet was extremely difficult to produce and was not consistent in the conditions in which one might be obtained. It should be noted that a distinction is made between a foamy, unsteady supercavity and a supercavity with a re-entrant jet at the tail. The foamy, unsteady cavity could be produced at every value of Froude number tested for ventilation rates up to critical value when the supercavity made the transition the long, twin vortex supercavity, while a stable, re-entrant jet supercavity was only seen in rare conditions. Figure 12 shows a comparison between the two at the same Froude number and different ventilation rates. The re-entrant jet at the rear of the cavity could be observed during the transition from a short, foamy cavity to a stable twin vortex supercavity, but was rarely stable. It was found that if the supercavity length was used as the characteristic length, then the product showed strong support for empirical data of Campbell et al. [12] with the product $\sigma_c Fr_l$ greater than one when a foamy, unsteady supercavity was present and less than one when a stable, twin vortex supercavity was observed.

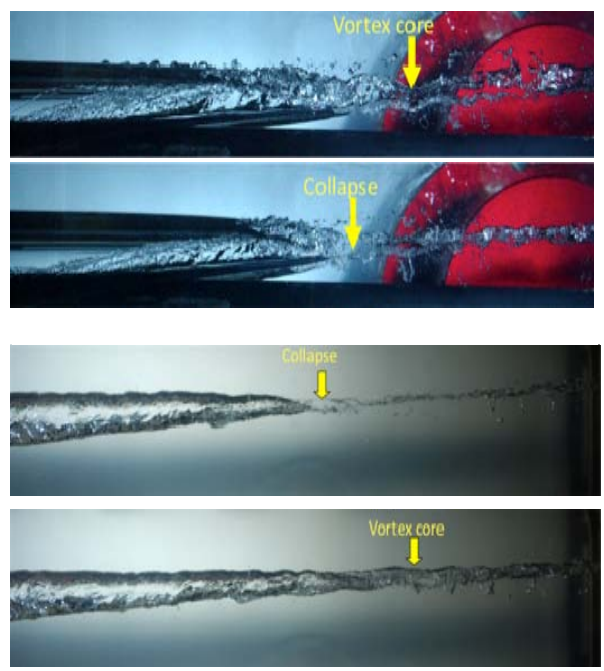

Figure 11. Examples of closure for both models. Top: forward facing model. Bottom: backward facing model.

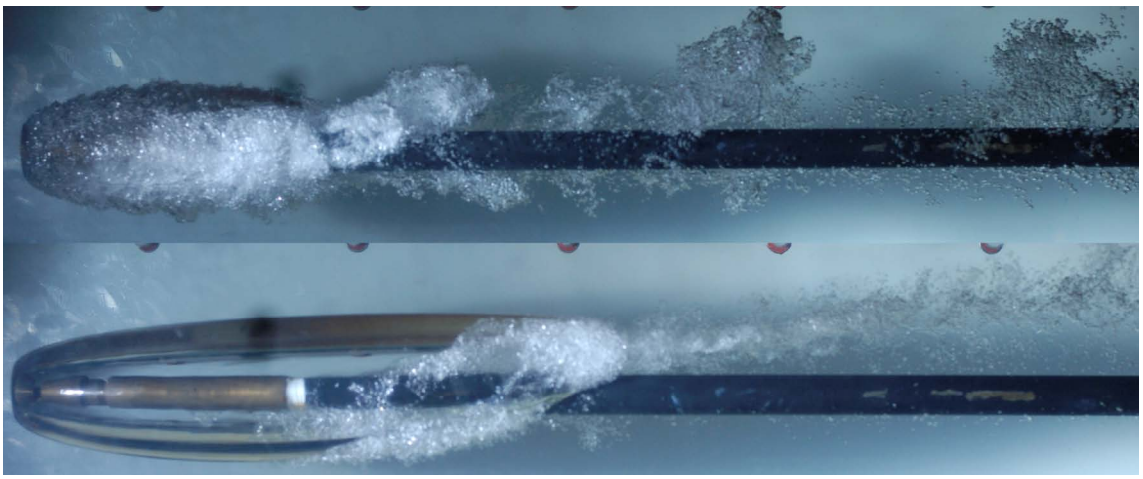

Figure 12. Comparison of short, foamy supercavity to re-entrant jet supercavity. Fr = 9 and d_c = 20mm. The top image corresponds to a ventilation rate lower than the critical value required to transition to a long, twin vortex supercavity. The lower image corresponds to a ventilation rate lower than the critical value to create a supercavity after a long, twin vortex supercavity had previously been formed, but not lower than the critical value to collapse the supercavity. The ventilated cavitation number for the lower image was 0.36, which was similar to values found when a long, twin vortex supercavity was present for the given conditions.

At low Froude numbers and small ventilation rates, a third mode of air entrainment was observed for both models. For these conditions, two sets of vortex pairs were present, one pair above the other (Figure 13). Just as with the single vortex pair, an ongoing process of a vortex core forming and collapsing was observed. For the two sets of vortex pairs, the pairs did not collapse simultaneously but at different times. Kapankin [9] predicted this method of gas entrainment to occur at cavitator angles greater than some critical angle. For the experiments conducted at SAFL, the cavitator was held at a zero degrees. The reason for the two sets of vortex pairs is not fully understood and will be further investigated.

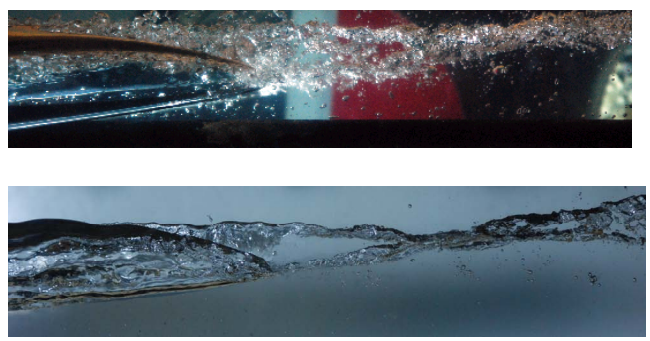

Figure 13. Example of quad-vortex. Top: forward facing model. Bottom: backward facing model. Note that the images are side views of the supercavity. Each vortex seen in the images (top and bottom) has a matching vortex behind it.

CONCLUSIONS

As seen by various researchers, the variation of Froude number significantly affects the minimum cavitation number seen (for cavitation numbers greater than the blockage value). As Froude number increases, the minimum cavitation number observed when a stable, twin vortex supercavity is present, decreases. The blockage ratio determines the lower limit for the cavitation number where a further increase in Froude number will not see a decrease in minimum cavitation number. As the ratio between the ventilated cavitation number and the cavitation number predicted based on blockage approached unity, numerical results from Tulin and Brennen can be used to compute cavitation number. The Froude number that this occurs at is less than infinite (assumption made by Brennen and Tulin). This is advantageous for configurations where direct measurement of pressure inside the supercavity is not possible. The minimum cavitation number for a given size cavitator is a function of the Froude number and the blockage ratio.

The presence of a body inside the supercavity serves to increase the required ventilation rate to create a stable supercavity, but does not appear to affect the method of gas removal. In contrast to the empirical observations of Campbell et al. [12], the product $\sigma_c Fr_d$ is consistently much greater than one even though twin vortex closure mechanism is dominant for stable supercavities for all configurations tested. If cavity length is used as the characteristic length instead of cavitator diameter, then $\sigma_c Fr_l < 1$ when twin vortices are the closure mechanism and $\sigma_c Fr_l > 1$ when an unsteady, foamy supercavity is present. A re-entrant jet supercavity was rarely found to be stable and was observed during the transition from a short, foamy supercavity to a long twin vortex supercavity. The reasons for this are not completely understood.

Froude number and blockage effects can account for the determination of the minimum cavitation number, but cannot account for the disagreement with closure mechanism predictions. This implies that there are more factors affecting the closure of the supercavity which are not fully understood.

NOMENCLATURE

d_c = diameter of cavitator (mm)
D = equivalent diameter of tunnel test section (cm)
D_c = maximum diameter of supercavity (mm)
L_c = cavity length (mm)
P_∞ = freestream pressure (Pa)
P_c = pressure inside supercavity (Pa)
P_v = vapor pressure of water (Pa)
U_∞ = freestream velocity (m/s)
U_c = velocity on the cavity surface (m/s)
ρ = density of water (kg/m^3)
g = acceleration due to gravity (m/s^2)
Q = volumetric flowrate of ventilation air (l/min)
β = Parameter for predicting presence of pulsating supercavity

Natural cavitation number σ_v: $$\sigma_v = \frac{P_\infty - P_v}{\frac{1}{2}\rho U_\infty^2}$$

Ventilation cavitation number σ_c: $$\sigma_c = \frac{P_\infty - P_c}{\frac{1}{2}\rho U_\infty^2}$$

Minimum cavitation number $\sigma_{\min}$: $$\sigma_c = \frac{P_\infty - P_{c,\max}}{\frac{1}{2}\rho U_\infty^2}$$

Froude number Fr: $$Fr = \frac{U_\infty}{\sqrt{g d_c}}$$

Froude number based on cavity length Fr_l: $$Fr_l = \frac{U_\infty}{\sqrt{g L_c}}$$

Air entrainment coefficient C_q: $$C_q = \frac{Q}{U_\infty d_c^2}$$

Blockage Ratio: $$\frac{D}{d_c}$$

ACKNOWLEGEMENTS

The Office of Naval Research supported this research. Dr. Ron Joslin is the contract monitor

REFERENCES

[1] Semenenko, V.N. "Artificial Supercavitation. Physics and Calculation," *Lecture Notes from the RTO AVT/VKI Special Course on Supercavitating Flows*, von Karman Institute for Fluid Dynamics, Rhode Saint Genèse , Belgium, 2001.

[2] Savchenko Y.N. "Experimental Investigation of Supercaviting Motion of Bodies", *Lecture Notes from the RTO AVT/VKI Special Course on Supercavitating Flows*, von Karman Institute for Fluid Dynamics, Rhode Saint Genèse , Belgium, 2001.

[3] Franc and Michel, *Fundamentals of Cavitation*, Kluwer Academic Publishers, Boston, MA, 2004.

[4] Paryshev, E.V. "Mathematical Modeling of Unsteady Cavity Flows", Fifth International Symposium on Cavitation (CAV 2003), Osaka, Japan, 2003.

[5] Wosnik, M. Schauer, T. Arndt, REA "Experimental Study on a Ventilated Vehicle", Fifth International Symposium on Cavitation (CAV2003), Osaka, Japan, 2003.

[6] Schauer, T. "An experimental study of a ventilated supercavity vehicle" Master of Science Thesis, University of Minnesota, 2003.

[7] Brennen, C. A numerical solution of axisymmetric cavity flows . J. Fluid Mechanics, 37, pp. 671-688, 1969.

[8] Tulin, M.P. Supercavitating Flows. In Streeter, V. (ed.), Handbook of Fluid Dynamics, McGraw-Hill, New York, pp. 1224 to 1246, 1961.

[9] Kapankin, Y.N., Gusev, A.V., Experimental Research of Joint Influence of Fluid and Lift Power of Cavitator on Character of Flow in Cavity Rear Part and Gas Departure from it, Proceedings of CAHI 1984. – No. 2244, Moscow, Russia, pp. 19-28, 1982

[10] Reichart, H. The Laws of Cavitation Bubbles at Axially Symmetrical Bodies in a Flow. Ministry of Aircraft Production (Great Britain), Reports and Translations No. 766, 1946.

[11] Waid, R.L. Cavity shapes for Circular Disks at Angles of Attack, Cal. Institute of Technology, Report No. E-73.4, 1957.

[12] Campbell I.J. & Hilborne D.V., Air entrainment behind artificially inflated cavities, *Proc. 2nd Int. Symp. On Naval Hydrodynamics,* Washington, D.C., 1958.